A neural correlate of working memory in the monkey primary visual cortex

Supèr, H.; Spekreijse, H.; Lamme, V.A.F.

Link to publication

Citation for published version (APA):
Supèr, H., Spekreijse, H., & Lamme, V. A. F. (2001). A neural correlate of working memory in the monkey primary visual cortex. *Science*, *293*(5527), 120-124. https://doi.org/10.1126/science.1060496

Tip60, and the second PTB domain, for binding to APP. For Tip60, both a partial rat cDNA and full-length human cDNA were analyzed (*22*).

29. J. Kamine, B. Elangovan, T. Subramanian, D. Coleman, G. Chinnadurai, *Virology* **216**, 357 (1996).
30. Q. Ran, O. M. Pereira-Smith, *Gene* **258**, 141 (2000).
31. T. Yamamoto, M. Horikoshi, *J. Biol. Chem.* **272**, 30595 (1997).
32. T. Ikura *et al.*, *Cell* **102**, 463 (2000).
33. The GST pull-down assays were performed essentially as described (*46*), by using purified wild-type and mutant rat GST-Tip60β, APP, and Myc-Fe65 expressed by transfection in COS cells. Extracts from transfected COS cells were incubated for 4 hr at 4°C with 10 μg of GST-Tip60 or GST-Tip60* bound to glutathione agarose. Beads were washed five times in 0.15 M NaCl, 50 mM Hepes-NaOH, pH 7.5, 1% IGEPAL CA-630 (Sigma) resuspended in 100 μl SDS-polyacrylamide gel electrophoresis (SDS-PAGE) sample buffer, and 20 μl were analyzed by SDS-PAGE and immunoblotting using antibodies to APP and the HA- and Myc-epitopes.
34. C. Zwahlen, S. C. Li, L. E. Kay, T. Pawson, J. D. Forman-Kay, *EMBO J.* **19**, 1505 (2000).
35. C. Dalluin *et al.*, *Mol. Cell* **6**, 921 (2000).
36. Y. Yan, N. A. Barlev, R. H. Haley, S. L. Berger, R. Marmorstein, *Mol. Cell.* **6**, 1195 (2000).
37. HeLa cells plated on cover glass in a 12-well plate were transfected with pcDNA3.1-N-HA-Fe65, pCM-VMyc-hTip60, and pCMV5-APP (0.2 μg each) using Fugene6 (Roche). Two days after transfection, cells were washed two times with PBS, fixed (3.7% formaldehyde for 10 min at room temperature), and blocked and permeabilized in PBS containing 3% bovine serum albumin, 0.1% IGEPAL CA-630 for 20 min. Cells were then incubated with mouse monoclonal antibody against HA (BabCo, Berkeley, CA), rabbit polyclonal antibody against APP, and goat polyclonal antibody against Myc (Santa Cruz Biotechnology, Santa Cruz, CA) for 1 hour, washed three times with PBS, and treated with the appropriate Cy2-, Cy3-, and Cy5-labeled secondary antibodies (Jackson Laboratories) for 1 hour. After three washes with PBS and one wash with water, cells were mounted and observed by microscopy.
38. G. Minopoli *et al.*, *J. Biol. Chem.* **276**, 6545 (2001).
39. For transactivation assays of Gal4-Tip60, COS, HeLa, and HEK293 cells were cotransfected with one of the following: (i) pG5E1B-luc (Gal4 reporter plasmid); (ii) pCMV-LacZ (β-galactosidase control plasmid); (iii) pMst (Gal4); pM-hTip60 (full-length wild-type human Gal4-Tip60β); or pM-hTip60* (full-length mutant human Gal4-Tip60β); (iv) pCMV5-Fe65 (Fe65), pCMVMyc-Fe65(242-711) [Fe65(242-711)], pCMV5-Fe65(1-553) (Fe65Δ PTB2), or pCMV5-Fe65mW4 (Fe65mW4) where indicated; and (v) pCMV5-APP (human APP695) or pCMV5-APP* (mutant human APP695). All transfections contained one of the plasmids listed in (i to iii), whereas (iv) and (v) were variable. Analyses were performed as described in (*19*).
40. M. S. Brown, J. Ye, R. B. Rawson, J. L. Goldstein, *Cell* **100**, 391 (2000).
41. Y. M. Chan, Y. N. Jan, *Cell* **94**, 423 (1998).
42. B. L. Sopher *et al.*, *Brain Res. Mol. Brain Res.* **26**, 207 (1994).
43. D. C. Lu *et al.*, *Nature Med.* **6**, 397 (2000).
44. A. B. Vojtek, S. M. Hollenberg, J. A. Cooper, *Cell* **74**, 205 (1993).
45. M. Okamoto, T. C. Südhof, *J. Biol. Chem.* **272**, 31459 (1997).
46. Y. Hata, C. A. Slaughter, T. C. Südhof, *Nature* **366**, 347 (1993).
47. X. Cao, T. Südhof, unpublished observations.
48. We thank C. Haass (Munich, Germany), N. Huang and W. Miller (UCSF), R. Roeder (Rockefeller University), J. Herz, E. Olson, J. Lu, M. Lush (University of Texas, Southwestern), K. Beyreuther (Heidelberg, Germany), and R. Jahn (Goettingen, Germany) for reagents and advice. We are grateful to S. Sisodia, M. S. Brown, J. L. Goldstein, E. H. Koo, and D. Selkoe for advice and discussions.

A Neural Correlate of Working Memory in the Monkey Primary Visual Cortex

Hans Supèr,[1,2]* Henk Spekreijse,[1] Victor A. F. Lamme[1,2]

The brain frequently needs to store information for short periods. In vision, this means that the perceptual correlate of a stimulus has to be maintained temporally once the stimulus has been removed from the visual scene. However, it is not known how the visual system transfers sensory information into a memory component. Here, we identify a neural correlate of working memory in the monkey primary visual cortex (V1). We propose that this component may link sensory activity with memory activity.

We trained monkeys (*Macaca mulatta*) to perform a delayed-response task in which the animals had to remember briefly the location of a figure after it had been removed from the visual scene (*1*). The animals fixated on a small central red dot on a computer screen (Fig. 1). After a 300-ms fixation, a motion-defined figure appeared very briefly (28 ms) at one of three locations (Fig. 1). After this stimulus had been presented, the animal had to continue fixating the central spot until it was switched off (Fig. 1A, "Cue time"). The removal of the fixation point indicated to the animal to make a saccade toward the position where the figure had been presented. The animal was rewarded only when fixation was maintained until the cue, and when the saccade was made to the correct position. The latency of the cue time was varied between 0 and 2000 ms after stimulus onset. Thus, while fixating, the animal had to remember the location of the briefly presented figure during a period of up to about 2 s. Detection of the figure was high and declined for longer delay periods (Fig. 2A), indicating that the task requires short-term memory processes.

During the delayed-response task, multiunit activity of V1 neurons was recorded in two monkeys (*2*). The display was filled with random dots. Stimulus onset thus evoked neural responses for "figure" [when the figure dots were overlying the V1 receptive fields (RFs)] as well as for "ground" motion (when the figure was presented elsewhere and background dots covered the RF) (Fig. 1C). We arranged the directions of motion such that, on average, the motion stimuli on the RF were identical for the "figure" and "ground" situations (*3, 4*).

The initial responses to figure and ground motion were identical up to about 70 ms after stimulus onset (Fig. 2B). At longer latencies, however, the response to figure motion was typically stronger than to background motion. This late enhancement of the sensory response—contextual modulation—correlates closely with the perception of the figure (*4–6*). Contextual modulation in V1 depends on feedback from higher visual areas (*7–9*), which implies that it is a specific correlate of recurrent processing. What happens to this modulation once the stimulus is no longer present, but has to be remembered?

During the delay period, the figure response remained stronger than the ground response (Fig. 2B) ($P < 10^{-4}$ for all delay periods). Thus, contextual modulation continues after the figure is removed from the visual field. In a control experiment, we observed the same phenomenon when a static, rather than a moving, stimulus was used in the same delayed-response task. Here, a static texture with an orientation-defined figure (*10*) was presented for 100 ms and followed by a mask containing a different texture, where the figure was no longer visible. Also in this experiment, contextual modulation continued during the whole period (900 ms) that the animal had to remember the figure location (Fig. 2E). Thus, the persistence of contextual modulation is not due to any peculiarity of the motion stimulus.

We calculated the strength of contextual modulation (*3*) for the first 250 ms after stimulus onset as an indication of the initial segregation strength of the figure from ground, and for the last 250 ms before cue time as an indication of the signal strength available for responding in the memory task. In the first part of the response, the strength of contextual modulation was similar for all

[1]Graduate School Neurosciences Amsterdam, Department of Visual System Analysis, Academic Medical Center, University of Amsterdam, Post Office Box 12011, 1100 AA Amsterdam, Netherlands. [2]The Netherlands Ophthalmic Research Institute, Meibergdreef 49, 1105 BA Amsterdam, Netherlands.

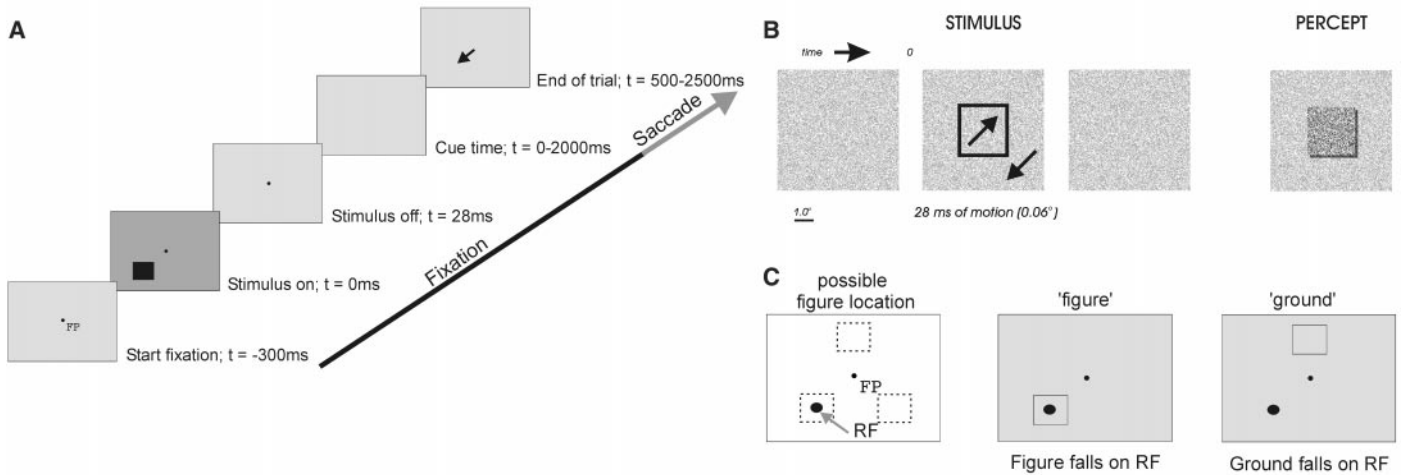*To whom correspondence should be addressed. E-mail: h.super@ioi.knaw.nl

Fig. 1. Experimental setup and illustration of a figure-ground display. (**A**) Animals were trained to fixate a central red spot (FP) on a stimulus screen filled with random dots. At stimulus onset a motion-defined figure (**B**) appeared for 28 ms. The animals maintained fixation for 0 to 2000 ms. After the offset of the fixation point (cue time), animals had to make a saccade toward the location where the figure had been presented (arrow in upper right panel). (**C**) The small circle indicates the locations of the receptive fields (RF). When the figure was overlying the RF, responses to "figure" were recorded. In the two other figure locations, "ground" responses were obtained.
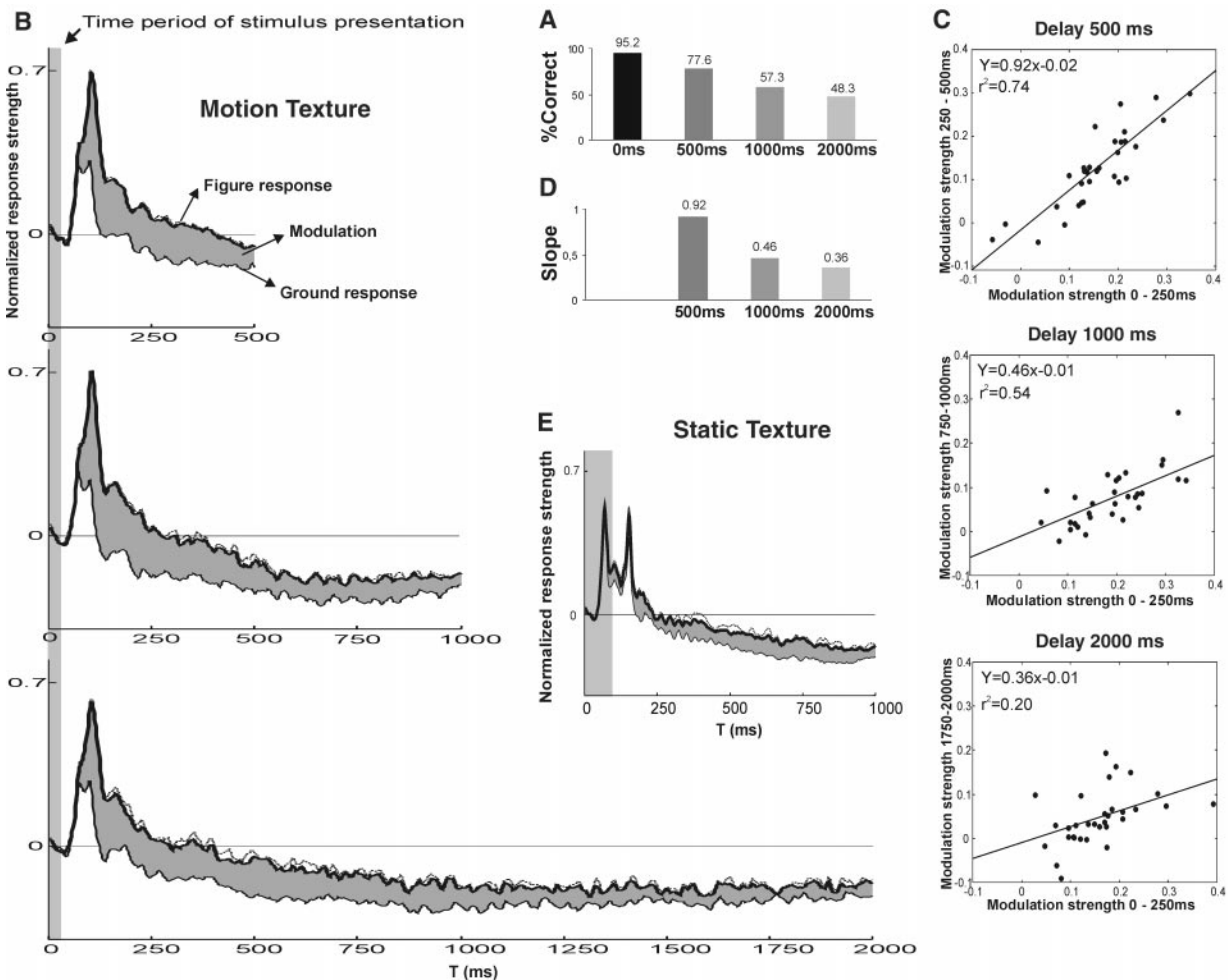

Fig. 2. Behavioral performance and neural responses in a delayed-response task with random dot motion–defined (**A** to **D**) and texture orientation–defined (**E**) figure-ground stimuli. (A) The percentage of correct trials for the different delay periods. (B) Neuronal responses (population average of all trials) to figure (thick lines) and to ground (thin lines). Contextual modulation is indicated by the shaded area. Dotted lines above the figure responses indicate the SEM. (C) Average modulation strength for the first 250-ms period after stimulus onset for each individual electrode is plotted against the average modulation strength of the 250-ms period before cue time. A linear regression curve is fitted through the data points. (D) Slopes of the regression curves in (C) for the different delay periods. Data of the 0-ms-delay period cannot be analyzed this way. (E) Neuronal responses for static figure-ground–defined texture. The first peak corresponds to the figure onset, and the second peak to figure offset/mask onset. Shading as in (B).

conditions. However, the strength of contextual modulation at subsequent stages decreased with increasing delay length. To quantify the decline in modulation strength with increasing delay length, we plotted the initial modulation strength of the first 250 ms after stimulus onset against the modulation strength of the last 250 ms before cue time for each individual recording unit (Fig. 2C). For the 1000- and 2000-ms delay periods, there was a significant decline in modulation ($P <$ 10^{-7}). We then fitted a linear regression line through these data points for each delayed-response period. The slope declined for longer delay periods (Fig. 2D). This indicates that the strength of contextual modulation is related to the delay period, where modulation becomes weaker for longer delays.

To establish a direct correlation between the persistence of modulation and memory performance, we analyzed the data according to the report of the animal, i.e., correct and incorrect responses. In correct trials, the animal made a saccade toward the figure location within 500 ms after cue time. In incorrect trials, the animal failed to respond correctly within this period. We then calculated the strength of contextual modulation for correct and incorrect responses separately. Contextual modulation was present during the first 250-ms period after stimulus onset for both the correct and incorrect trials (Fig. 3). Subsequently, the average strength of contextual modulation decreased in the later parts of the delay period. The decrease of modulation was stronger for incorrect trials, and contextual modulation for the incorrect trials disappeared completely in the late part of the delay period (Fig. 3, B and D), whereas modulation for the correct trials continued (Fig. 3, A and C). Analysis of individual recording sites (Fig. 3, E and F) showed that the strength of the figure-ground signal during the first 250 ms after stimulus onset was similar for the correct and incorrect trails ($P > 0.1$ for both delay periods), but that most electrodes showed stronger modulation at the final 250 ms before cue time for correct trials compared with incorrect trials ($P < 10^{-5}$ for both delay periods). Dividing the average modulation strength of the last 250 ms before cue time by the modulation strength of the first 250-ms period after stimulus onset gives the relative degree of modulation persistence during the delay period (Fig. 3, G and H). This persistence is much weaker (and in fact negative) for incorrect than for correct trials ($P < 0.005$ for both delay periods).

Thus, for correct trials as well as for incorrect trials, the figure is equally well segregated from the ground, as indicated by the presence of contextual modulation in the first 250 ms after stimulus onset. However, during the delay period, modulation continues for correct trials and disappears
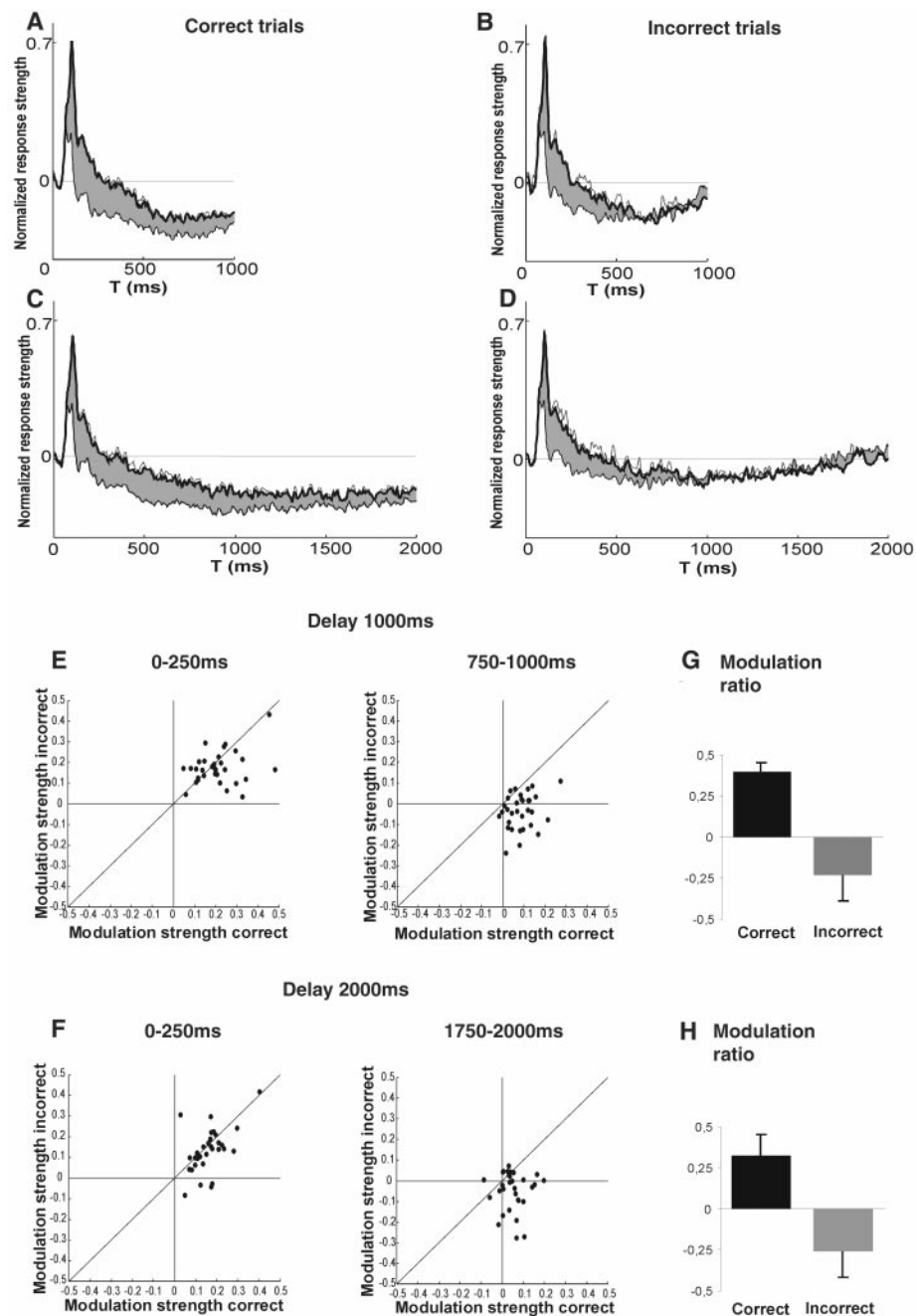

Fig. 3. Neurophysiological responses and modulation strength for the 1000- and 2000-ms-delay period sorted according to behavioral result. (**A** to **D**) The population average neural activity for figure and ground for correct [(A) and (C)] and incorrect trials [(B) and (D)]. Shading as in Fig. 2. (**E** and **F**) Modulation strength during the given intervals of each recording unit for correct trials versus incorrect trials. (**G** and **H**) Population average of modulation ratios (modulation strength during the first 250 ms divided by modulation during the last 250 ms) for correct and incorrect trials.

completely for incorrect trials.

Another important feature of working memory is that relevant information is actively stored for later use, i.e., the information is stored only if necessary (*11*). To test whether the sustained modulation that we observed was an active process, we presented a second stimulus during the delay period (Fig. 4, A and B). The second stimulus appeared 500 ms after the onset of the first stimulus and

remained on the screen until the end of the trial. The second stimulus could be either relevant or irrelevant to the delayed-response task. In the figure = target condition, the animals had to saccade to the remembered position of the first stimulus (as before), and the second stimulus was irrelevant. In the figure = distractor condition, the animals had to remember the position of the second stimulus, and the figure was irrelevant (*12*).
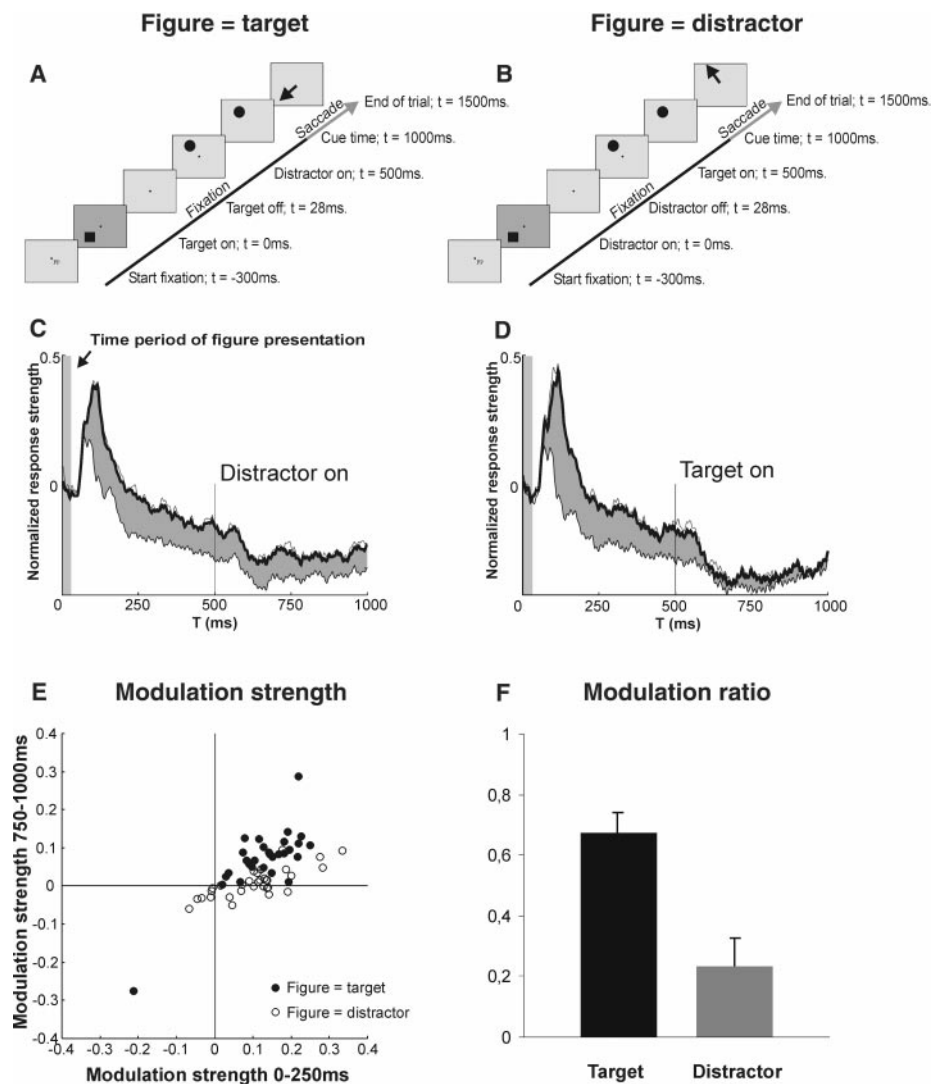
Fig. 4. Experimental setup and figure-ground responses for a 1000-ms delayed-response task where the figure was either target or distractor. (**A** and **B**) The delayed-response task was as described in Fig. 1 except that a second stimulus (circle) was presented 500 ms after the figure onset (square). After the offset of the fixation point, animals had to make a saccade toward the figure location in the figure = target condition (A) or toward the second stimulus (circle) in the figure = distractor condition (arrows in upper right panels). (**C** and **D**) The average figure-ground responses for figure = target condition (C) and figure = distractor condition (D). Shading as in Fig. 2. (**E**) Strength of modulation for the 250-ms period after figure onset versus strength of modulation for the 250-ms period before cue time of each recording unit for the figure = target condition (solid circles) and for the figure = distractor condition (open circles). (**F**) Population average of modulation ratios (see Fig. 3, G and H) for the figure = target and figure = distractor conditions.

In both conditions, contextual modulation was present before the onset of the second stimulus (Fig. 4, C to E) (difference in modulation strength $P > 0.1$). The appearance of the second stimulus had a strong nonspecific effect on the activity of the recorded neurons, where the average responses to both figure and ground decreased after the onset of the second stimulus (Fig. 4, C and D). However, a very task-specific effect was observed on the difference between figure and ground responses: Contextual modulation continued in trials when the figure was the target, whereas it decreased when the figure was

the distractor (Fig. 4, C and D). Again, we quantified the initial (0 to 250 ms) and the final (750 to 1000 ms) amount of modulation for each individual electrode (Fig. 4E), and calculated the relative degree of persistence of modulation during the delay period (Fig. 4F). The remaining amount of modulation is much stronger when the figure is relevant to the memory task than when it is not ($P < 0.0005$). These results indicate that the continuation of modulation is not a passive process but is related to an active storage of information needed for the animal's goal.

In the primary visual cortex, neural activ-

ity related to figure-ground segregation thus continues during the delay period in a memory guided task (Fig. 2). The persistence of figure-ground modulation is stronger when the task is performed correctly (Fig. 3) and when the figure evoking the modulation is relevant to the task (Fig. 4). The continued figure-ground signal is accompanied by an overall reduction in activity (see Figs. 2 to 4). Thus, whereas one mechanism suppresses overall activity in V1 during the delay, another mechanism seems to be able to maintain the difference in figure versus ground signals. In that sense, the maintained activity is different from delay-period activity recorded in temporal (*13*) or prefrontal (*14*) cortex. This difference may also explain why in functional magnetic resonance imaging studies, very little delay activation is found in early visual areas (*15*).

It is highly unlikely that the maintained activity is a neural correlate of visual persistence, i.e., the lasting visibility of a stimulus after its physical disappearance. In humans, visual persistence for motion-defined stimuli has been shown to last 40 to 130 ms after stimulus offset (*16*, *17*). However, our data show that contextual modulation is present for up to 2 s after the removal of the figure (Fig. 2B). Maintained modulation occurs even when the display is replaced with a different stimulus (Fig. 2E).

Instead, our results show a strong correlation between the active and successful storage of information about (the location of) the stimulus and the maintained figure-ground signal. Whereas the first part of this activity may thus be related to the perceptual experience of the figure segregating from ground [see also (*5*, *6*)], the later part is more likely related to a memory trace of the stimulus (*11*, *13*). We therefore propose that contextual modulation in the primary visual cortex is a correlate of the process that forms a bridge between sensory activity and working memory.

References and Notes
1. Two monkeys were trained to fixate at a point on the monitor and to maintain fixation for 0 to 2000 ms. After cue time, which was the offset of the fixation point, the monkey had to saccade toward the figure location. The maximum time allowed for responding to the figure location was 500 ms. Trials where eye position left the fixation window (1° by 1°) before cue time were discarded. Eye movements were monitored by using scleral search coils (*5*). Stimuli were presented on a 21-inch monitor screen (28° by 21° of visual angle, resolution 1024 by 768 pixels, refresh rate 72.34 Hz). In each trial, a red fixation spot (0.2°) popped up in a prestimulus texture consisting of random pixels with a 50% probability of being either black or white. After the monkey had fixated this spot for 300 ms, the random dots were moved very briefly (28 ms, i.e., two video frames) and over a very short distance (two pixels, 0.06°). Motion onset was considered stimulus onset. The direction of movement of the dots was 45°, 135°, 225°, or 315°. The movement of a square "figure" region (3° of visual angle) was always 180° opposite to that

of the background. Motion-defined figures could (randomly) appear at one of three possible locations (eccentricity. 2.7° to 4.4°),

2. Multiunit activity was recorded through 16 microwire electrodes in each monkey (4, 6). Receptive-field size ranged from 0.7° to 1.4° (median 0.9°), and eccentricity from 1.3° to 2.8° in one monkey and from 3.4° to 5.7° in the other. For each monkey, figure positions and electrodes were chosen such that the figures covered the receptive fields of 16 electrodes simultaneously.

3. Data were obtained in pseudo-randomly interleaved blocks of trials in 9 to 12 daily sessions. To ensure identical receptive-field stimulation for figure and background responses, we compared the responses to the same directions of motion for figure and ground and averaged the responses to the different directions of motion. Electrophysiological data obtained during the interval between stimulus onset and cue time were analyzed. Response strength was calculated as the average normalized activity during the intervals. Contextual modulation was calculated by subtracting the background response strength from

the figure response strength. For all statistics, paired t tests were applied.

4. V. A. F. Lamme, K. Zipser, H. Spekreijse, *Proc. Natl. Acad. Sci. U.S.A.* **95**, 3263 (1998).
5. V. A. F. Lamme, H. Supèr, R. Landman, P. R. Roelfsema, H. Spekreijse, *Vision Res.* **40**,1507 (2000).
6. H. Supèr, H. Spekreijse, V. A. F. Lamme, *Nature Neurosci.* **4**, 304 (2001).
7. J. M. Hupé *et al.*, *Nature* **394**, 784 (1998).
8. V. A. F. Lamme, H. Spekreijse, H. Spekreijse, *Curr. Opin. Neurobiol.* **8**, 529 (1998).
9. B. R. Payne, S. G. Lomber, A. E. Villa, J. Bullier, *Trends. Neurosci.* **19**, 535 (1996).
10. For the static figure-ground texture, we used line segments that were 16 by 1 pixels (0.44° by 0.027°) and the density was five line segments per square degree. Two different line segment orientations (135° or 45°) were used to segregate figure from ground, and both line orientations were used for figure and background.
11. J. M. Fuster, *Trends. Neurosci.* **20**, 451 (1997).
12. The motion defined figure-ground display was identical to that described before, except that during the delay period a second stimulus (red circle: size 2° to 3°, eccentricity: 5.5° to 6°) appeared in one of three positions but different from that of the figure location. For this task, another monkey was also used. Data were obtained in blocked 10 to 12 daily sessions and normalized as described in (3).
13. Y. Miyashita, H. S. Chang, *Nature*, **331**, 68 (1988).
14. P. S. Goldman-Rakic, in *Progress in Brain Research*, H. B. M. Uylings, C. G. P. van Eden, J. P. C. D. de Bruin, M. A. Corner, M. G. P. Feenstra, Eds. (Elsevier, Amsterdam, 1990), pp. 313–323.
15. S. M. Courtney, L. G. Ungerleider. K. Keil, J. V. Haxby, *Nature* **386**, 608 (1997).
16. V. Di Lollo, *J. Exp. Psychol. Hum. Percept. Perform.* **10**, 144 (1984).
17. S. Shiori, P. Cavanagh, *Vision Res.* **32**, 943 (1992).
18. We thank K. Brandsma and J. de Feiter for biotechnical support, and P. Brassinga and H. Meester for technical assistance. H.S. is supported by a grant of Medical Science (MW) from Netherlands Organization for Scientific Research (NWO).

Stimulation of RNA Polymerase II Elongation by Hepatitis Delta Antigen

Yuki Yamaguchi,[1] Julija Filipovska,[2] Keiichi Yano,[3]
Akiko Furuya,[3] Naoto Inukai,[1] Takashi Narita,[1] Tadashi Wada,[1]
Seiji Sugimoto,[3] Maria M. Konarska,[2] Hiroshi Handa[1]*

Transcription elongation by RNA polymerase II (RNAPII) is negatively regulated by the human factors DRB-sensitivity inducing factor (DSIF) and negative elongation factor (NELF). A 66-kilodalton subunit of NELF (NELF-A) shows limited sequence similarity to hepatitis delta antigen (HDAg), the viral protein required for replication of hepatitis delta virus (HDV). The host RNAPII has been implicated in HDV replication, but the detailed mechanism and the role of HDAg in this process are not understood. We show that HDAg binds RNAPII directly and stimulates transcription by displacing NELF and promoting RNAPII elongation. These results suggest that HDAg may regulate RNAPII elongation during both cellular messenger RNA synthesis and HDV RNA replication.

The human transcription elongation factors DSIF and NELF bind RNAPII and repress the elongation activity of this polymerase (1–4). This repression is reversed by P-TEFb, a positive elongation factor with a protein kinase activity that phosphorylates the COOH-terminal domain (CTD) of RNAPII and a subunit of DSIF (5), in a manner sensitive to the kinase inhibitors 5,6-dichloro-1-beta-D-ribofuranosylbenzimidazole (DRB) and H8. Because DRB affects the synthesis of most mRNAs, the DRB-sensitive elongation involving DSIF, NELF, and P-TEFb may reflect a general rate-limiting step of RNAPII transcription (6). The yeast homologs of

DSIF, transcription factors Spt5 and Spt4, have been shown to affect elongation (7). Purified NELF is composed of five polypeptides, A to E, the smallest of which, NELF-E (46 kD), is identical to a putative RNA-binding protein (4). We microsequenced NELF-A (66 kD) and found it to be encoded by *WHSC2* (Fig. 1A), a candidate gene for the Wolf-Hirschhorn syndrome, a multiple malformation syndrome characterized by mental and developmental defects resulting from a deletion in chromosome 4p16.3 (8). Computer analyses identified a weak sequence similarity (27% identity) between the NH_2-terminal half of NELF-A/WHSC2 (amino acids 89 to 248) and HDAg, the sole protein encoded by HDV, with the similarity extending to the predicted secondary structures of these proteins (Fig. 1B).

HDV, a satellite of hepatitis B virus, has a ~1700-nucleotide (nt) circular, single-stranded RNA genome with a rodlike structure (9). Replication of HDV RNA appears to involve the

host RNAPII and requires the presence of HDAg (9–11). Two forms of HDAg, HDAg-S (195 amino acids long) and HDAg-L (214 amino acids long), originate from editing of the common mRNA. Both forms bind HDV RNA, but have distinct roles in the viral life cycle. HDAg-S activates HDV replication, whereas HDAg-L, which contains a 19–amino acid COOH-terminal extension, inhibits replication and directs virion assembly (9–12). Earlier reports have implicated HDAgs in both activation and inhibition of RNAPII transcription (13, 14), but the nature of this discrepancy and the mechanism of HDAg action are unknown.

To investigate if, and how, HDAgs regulate RNAPII transcription, we examined the effect of HDAg on DNA-templated transcription using HeLa nuclear extracts (NE). In the presence of DRB, endogenous DSIF/NELF can repress transcription (Fig. 2A) (4). HDAgs reversed this inhibition (HDAg-S was more effective than HDAg-L), with little effect on basal (–DRB) transcription (Fig. 2A). This effect required NELF, because NE immunodepleted of NELF failed to respond to HDAgs (Fig. 2B). These results suggest that HDAg stimulates RNAPII transcription by counteracting the negative effect of DSIF/NELF.

Because HDAg does not affect the kinase activity of P-TEFb or CTD phosphorylation (15), we sought to determine whether it affects association of NELF, DSIF, and RNAPII under transcription conditions. In NE prepared from HeLa cells expressing Flag–NELF-E, antibodies to Flag (anti-Flag) immunoprecipitated the other NELF subunits (15), DSIF, and RNAPII (Fig. 3A) (4). Preincubation of the NE with HDAg-S substantially reduced the levels of DSIF and RNAPII in the precipitate (Fig. 3A), but had little effect on DSIF-RNAPII interaction (15). To determine the direct target of HDAg, we analyzed the NE proteins associated with glutathione S-transferase (GST)–HDAg. Under

[1]Frontier Collaborative Research Center, Tokyo Institute of Technology, 4259 Nagatsuta, Yokohama 226–8503, Japan. [2]Rockefeller University, New York, NY 10021, USA. [3]Tokyo Research Laboratories, Kyowa Hakko Kogyo, Machida, Tokyo 194–8533, Japan.

*To whom correspondence should be addressed. E-mail: hhanda@bio.titech.ac.jp